Multichannel Active Noise Control with Exterior Radiation Suppression Based on Riemannian Optimization

Takaaki Kojima
Faculty of Engineering, The University of Tokyo
Tokyo, Japan
kojima-takaaki@g.ecc.u-tokyo.ac.jp

Kazuyuki Arikawa
Graduate School of Information Science and Technology, The University of Tokyo
Tokyo, Japan

Shoichi Koyama
Digital Content and Media Sciences Research Division, National Institute of Informatics
Tokyo, Japan

Hiroshi Saruwatari
Graduate School of Information Science and Technology, The University of Tokyo
Tokyo, Japan

***Abstract*—A multichannel active noise control (ANC) method with exterior radiation suppression is proposed. When applying ANC in a three-dimensional space by using multiple microphones and loudspeakers, the loudspeaker output can amplify noise outside a region of target positions because most of current ANC methods do not take into consideration the exterior radiation of secondary loudspeakers. We propose a normalized least mean square algorithm for feedforward ANC in the frequency domain based on the Riemannian optimization to update the control filter with the exterior radiation power constrained to a target value. The advantages of the proposed method, compared with the algorithm using a penalty term of exterior radiation, were validated by numerical experiments: the exterior radiation power can be constrained during the adaptation process and the parameter for the constraint can be determined in advance.**

***Index Terms*—active noise control, adaptive filtering, exterior radiation suppression, Riemannian optimization**

I. Introduction

The goal of active noise control (ANC) is to cancel unwanted noise from primary noise sources using secondary loudspeakers. In typical multichannel feedforward ANC systems, the driving signals of the secondary loudspeakers to reduce noise at positions of error microphones, i.e., *target positions*, are obtained from reference microphone signals by filtering through a control filter adaptively optimized on the basis of error microphone signals. Although ANC techniques have been studied for several decades [1]–[3], their application to a three-dimensional (3D) space has recently attracted attention again because of recent advancements on spatial ANC techniques [4]–[7].

When applying the ANC techniques in a 3D space, an exterior region of target positions for noise reduction is normally not taken into consideration. Therefore, the noise outside the region of target positions can be largely amplified owing to secondary loudspeaker outputs. Several attempts have been made to suppress the output power of secondary loudspeakers [8]–[11]; however, the reduction in output power does not always lead to the suppression of exterior radiation.

For the above reasons, it is important to develop a multichannel ANC method to suppress the exterior radiation power of secondary loudspeakers while reducing noise at the target positions. The exterior radiation power can be formulated with their given directivity patterns [12]. In our previous study [13], normalized least mean square (NLMS)-based adaptive filtering algorithms for feedforward ANC in the frequency domain are derived with a penalty term or an inequality constraint on this exterior radiation formulation in the context of spatial ANC. To adapt the constraint on the external radiation power to the primary noise amplitude with the alleviation of the effect on the ANC performance, the NLMS algorithm derived from the cost function with an additive penalty term for exterior radiation power can be used. However, this algorithm has several issues in practice: 1) the exterior radiation power is not necessarily suppressed during the adaptation process even when its target value is successfully reached after convergence and 2) it is difficult to determine the parameter for balancing the penalty term before the adaption process.

We propose an NLMS-based multichannel feedforward ANC algorithm in the frequency domain based on the Riemannian optimization [14], [15], which can be regarded as an application of stochastic gradient descent on Riemannian manifolds [16]. The optimization problem for computing the control filter is defined as the minimization problem of noise at the target positions with an equality constraint on the exterior radiation power. We developed an NLMS algorithm to update the control filter on a Riemannian manifold constructed by the equality constraint. We conducted numerical experiments to evaluate the performance of the proposed method.

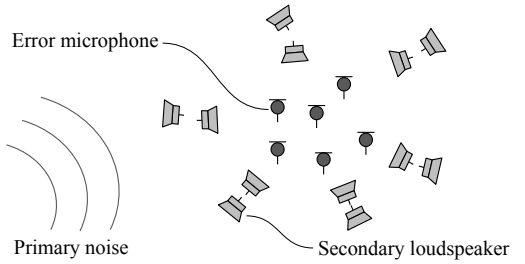

Fig. 1. Multichannel ANC in 3D space using multiple microphones and loudspeakers.

II. Multichannel ANC

Suppose that L secondary loudspeakers and M error microphones are placed in a 2D or 3D acoustic space, i.e., $\mathbb{R}^2$ or $\mathbb{R}^3$, as shown in Fig. 1. R reference microphones are placed near primary noise sources. The observed signals of the error and reference microphones, and the driving signals of the secondary loudspeakers at time frame n and angular frequency ω are denoted by $\boldsymbol{e}_n(\omega) \in \mathbb{C}^M$, $\boldsymbol{x}_n(\omega) \in \mathbb{C}^R$, and $\boldsymbol{y}_n(\omega) \in \mathbb{C}^L$, respectively. By denoting the primary noise at error microphone positions as $\boldsymbol{d}_n(\omega) \in \mathbb{C}^M$, we express the error microphone signals as

$$\begin{aligned}\boldsymbol{e}_n(\omega) &= \boldsymbol{d}_n(\omega) + \boldsymbol{G}(\omega)\boldsymbol{y}_n(\omega) \\ &= \boldsymbol{d}_n(\omega) + \boldsymbol{G}(\omega)\boldsymbol{W}_n(\omega)\boldsymbol{x}_n(\omega),\end{aligned} \tag{1}$$

where $\boldsymbol{G}(\omega) \in \mathbb{C}^{M\times L}$ is the transfer function matrix from secondary loudspeakers to error microphones and $\boldsymbol{W}_n(\omega) \in \mathbb{C}^{L\times R}$ is the adaptive control filter to obtain the optimal driving signals from the reference signals. Hereafter, the argument ω is omitted for notational simplicity.

The cost function of the multichannel ANC is generally defined as the expectation value of the power of error signals:

$$J = \mathbb{E}[\sigma_n(\boldsymbol{W}_n)] \tag{2}$$

with

$$\sigma_n(\boldsymbol{W}_n) := \|\boldsymbol{d} + \boldsymbol{G}\boldsymbol{W}_n\boldsymbol{x}_n\|_2^2 + \gamma\|\boldsymbol{W}_n\boldsymbol{x}_n\|_2^2, \tag{3}$$

and a regularization parameter $\gamma > 0$. By replacing the expectation value of σ_n with the instantaneous value in (2), i.e., $J \approx \sigma_n(\boldsymbol{W}_n)$, the NLMS algorithm for updating $\boldsymbol{W}_n$ is derived as

$$\begin{aligned}\boldsymbol{W}_{n+1} &= \boldsymbol{W}_n - \mu_n \frac{\partial \sigma_n}{\partial \boldsymbol{W}_n^*} \\ &= \boldsymbol{W}_n - \mu_n(\boldsymbol{G}^{\mathsf{H}}\boldsymbol{e}_n + \gamma\boldsymbol{W}_n\boldsymbol{x}_n)\boldsymbol{x}_n^{\mathsf{H}},\end{aligned} \tag{4}$$

with the step size parameter [17]

$$\mu_n = \frac{\mu_0}{\|\boldsymbol{G}^{\mathsf{H}}\boldsymbol{G} + \gamma\boldsymbol{I}_L\|_2\|\boldsymbol{x}_n\|_2^2}. \tag{5}$$

Here, $\boldsymbol{I}_L$ is the identity matrix of size $L \times L$ and $\mu_0 \in (0, 2)$ is a normalized step size parameter. $(\cdot)^*$ and $(\cdot)^{\mathsf{H}}$ denote the complex conjugate and conjugate transpose, respectively.

III. Exterior Radiation Suppression with Penalty Term

We introduce a multichannel ANC method to suppress the exterior radiation power while reducing noise, which is proposed in [13] in the context of spatial ANC.

First, the exterior radiation power of the secondary loudspeakers is formulated. Let $\partial\Omega$ be a surface of a circular or spherical area including all the secondary loudspeakers. The total acoustic power radiated from $\partial\Omega$ by all the secondary loudspeakers, that is, the exterior radiation power, is defined for the pressure field $u_n(\boldsymbol{r})$ generated by the nth-frame driving signals of the secondary loudspeakers as [12]

$$\varepsilon_n(\boldsymbol{W}_n) := \int_{\partial\Omega} \frac{1}{2}\mathrm{Re}\left[u_n(\boldsymbol{r})\frac{\mathrm{j}}{\rho ck}\frac{\partial u_n(\boldsymbol{r})^*}{\partial \boldsymbol{n}}\right]\mathrm{d}\boldsymbol{r}, \tag{6}$$

where ρ is the medium density, c is the speed of sound, $k := \omega/c$ is the wave number, and $\partial/\partial\boldsymbol{n}$ denotes the normal derivative on $\partial\Omega$. By representing $u_n(\boldsymbol{r})$ with the nth-frame driving signals $\boldsymbol{y}_n$, $\varepsilon_n(\boldsymbol{W}_n)$ is reformulated with a Hermitian matrix $\boldsymbol{A} \in \mathbb{C}^{L\times L}$ as

$$\varepsilon_n(\boldsymbol{W}_n) = \boldsymbol{y}_n^{\mathsf{H}}\boldsymbol{A}\boldsymbol{y}_n = \boldsymbol{x}_n^{\mathsf{H}}\boldsymbol{W}_n^{\mathsf{H}}\boldsymbol{A}\boldsymbol{W}_n\boldsymbol{x}_n. \tag{7}$$

When all the secondary loudspeakers are point sources, the (l, l')th element of $\boldsymbol{A}$ can be expressed as [12]

$$(\boldsymbol{A})_{l,l'} = \begin{cases} \dfrac{1}{8c\rho k}J_0(k\|\boldsymbol{r}_l - \boldsymbol{r}_{l'}\|_2) & \text{in 2D space} \\ \dfrac{1}{8c\rho k}j_0(k\|\boldsymbol{r}_l - \boldsymbol{r}_{l'}\|_2) & \text{in 3D space} \end{cases}, \tag{8}$$

where $\boldsymbol{r}_l$ is the position of the lth secondary loudspeaker, and $J_0(\cdot)$ and $j_0(\cdot)$ are 0th-order Bessel function and 0th-order spherical Bessel function, respectively. Note that ε_n corresponds to the power of the driving signals of the secondary loudspeakers when $\boldsymbol{A}$ is $\boldsymbol{I}_L$.

A simple strategy to suppress the exterior radiation power while reducing noise at the error microphone positions is to define the cost function as the weighted sum of σ_n and ε_n as follows [13]:

$$J_{\mathrm{Penal}} = \sigma_n(\boldsymbol{W}_n) + \lambda\varepsilon_n(\boldsymbol{W}_n), \tag{9}$$

where $\lambda > 0$ is the parameter used to determine the balance of the two terms. We here defined J_{Penal} as the instantaneous value instead of the expectation value as in the NLMS algorithm (4). The NLMS algorithm for minimizing J_{Penal} is derived similarly as

$$\boldsymbol{W}_{n+1} = \boldsymbol{W}_n - \mu_n[\boldsymbol{G}^{\mathsf{H}}\boldsymbol{e}_n + (\gamma\boldsymbol{I}_L + \lambda\boldsymbol{A})\boldsymbol{W}_n\boldsymbol{x}_n]\boldsymbol{x}_n^{\mathsf{H}}, \tag{10}$$

with the step size parameter

$$\mu_n = \frac{\mu_0}{\|\boldsymbol{G}^{\mathsf{H}}\boldsymbol{G} + \gamma\boldsymbol{I}_L + \lambda\boldsymbol{A}\|_2\|\boldsymbol{x}_n\|_2^2}. \tag{11}$$

IV. Proposed Algorithm Based on Riemannian Optimization

A. Riemannian Optimization for Exterior Radiation Suppression

The NLMS algorithm with a penalty term of the exterior radiation power presented in Sect. III has several issues in practice. First, although the exterior radiation can be suppressed after the convergence of the adaptive filter, there is no guarantee that the exterior radiation is suppressed during the adaptation process. Second, it is not simple to determine an appropriate parameter λ because it is difficult to explicitly relate the exterior radiation power after convergence with the parameter λ.

To overcome the above issues, we propose an NLMS algorithm based on the Riemannian optimization with an equality constraint on the exterior radiation power. We define the optimization problem as

$$\begin{aligned} &\underset{\boldsymbol{W}\in\mathbb{C}^{L\times R}}{\text{minimize}} \quad \sigma_n(\boldsymbol{W}) \\ &\text{subject to} \quad \boldsymbol{W}^{\mathsf{H}}\boldsymbol{A}\boldsymbol{W} = C\boldsymbol{I}_R, \end{aligned} \tag{12}$$

where $C > 0$. Again, the optimization problem is defined with the instantaneous value instead of the expectation value. By using this equality constraint, we can constrain the exterior radiation power proportional to the power of the reference microphones as

$$\varepsilon_n(\boldsymbol{W}) = \boldsymbol{x}_n^{\mathsf{H}}\boldsymbol{W}_n^{\mathsf{H}}\boldsymbol{A}\boldsymbol{W}_n\boldsymbol{x}_n = C\|\boldsymbol{x}_n\|_2^2. \tag{13}$$

We represent the equality constraint in (12) as a Riemannian manifold $\mathcal{M}$ on which the control filter $\boldsymbol{W}$ is updated:

$$\mathcal{M} := \{\boldsymbol{W} \in \mathbb{C}^{L\times R} \mid \boldsymbol{W}^{\mathsf{H}}\tilde{\boldsymbol{A}}\boldsymbol{W} = \boldsymbol{I}_R\}, \tag{14}$$

where $\tilde{\boldsymbol{A}} := \boldsymbol{A}/C$. Thus, the adaptive algorithm is obtained for the unconstrained minimization problem of $\sigma_n(\boldsymbol{W})$ on $\mathcal{M}$.

B. Derivation of NLMS algorithm

The control filter $\boldsymbol{W}$ is regarded as a point on a generalized Stiefel manifold $\mathcal{M}$. By defining an appropriate Riemannian metrics for $\mathcal{M}$, we obtain the gradient of the cost function, $\text{grad}\ \sigma_n(\boldsymbol{W}) \in T_{\boldsymbol{W}}\mathcal{M}$, as an orthogonal projection of the standard gradient $\partial\sigma_n(\boldsymbol{W})/\partial\boldsymbol{W}^*$ onto the tangent space of $\mathcal{M}$ at $\boldsymbol{W}$, denoted by $\mathcal{T}_{\boldsymbol{W}}\mathcal{M}$ [14]. To update $\boldsymbol{W}$ in the steepest descent direction, an approximate mapping called retraction is used [14].

The orthogonal projection of $\boldsymbol{U} \in \mathcal{T}_{\boldsymbol{W}}\mathbb{C}^{L\times R}$ onto $\mathcal{T}_{\boldsymbol{W}}\mathcal{M}$ is defined as [18]

$$\mathcal{P}_{\boldsymbol{W}}(\boldsymbol{U}) = \boldsymbol{U} - \tilde{\boldsymbol{A}}\boldsymbol{W}\boldsymbol{H}, \tag{15}$$

where $\boldsymbol{H}$ is the unique solution of the following Sylvester equation [19]:

$$\begin{aligned} (\boldsymbol{W}^{\mathsf{H}}\tilde{\boldsymbol{A}}^{\mathsf{H}}\tilde{\boldsymbol{A}}\boldsymbol{W})\boldsymbol{H} + \boldsymbol{H}(\boldsymbol{W}^{\mathsf{H}}\tilde{\boldsymbol{A}}^{\mathsf{H}}\tilde{\boldsymbol{A}}\boldsymbol{W}) \\ = \boldsymbol{W}^{\mathsf{H}}\tilde{\boldsymbol{A}}\boldsymbol{U} + \boldsymbol{U}^{\mathsf{H}}\tilde{\boldsymbol{A}}\boldsymbol{W}. \end{aligned} \tag{16}$$

Then, the gradient of the cost function is represented as

$$\text{grad}\ \sigma_n(\boldsymbol{W}) = \mathcal{P}_{\boldsymbol{W}}\left(2(\boldsymbol{G}^{\mathsf{H}}\boldsymbol{e}_n + \gamma\boldsymbol{W}\boldsymbol{x}_n)\boldsymbol{x}_n^{\mathsf{H}}\right). \tag{17}$$

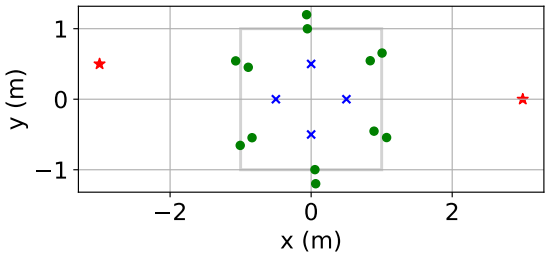

Fig. 2. Experimental settings. Blue crosses, green dots, and red stars indicate error microphones, secondary loudspeakers, and primary noise sources, respectively.

Next, a retraction at $\boldsymbol{W} \in \mathcal{M}$ from $\boldsymbol{V} \in \mathcal{T}_{\boldsymbol{W}}\mathcal{M}$ can be defined as [20]

$$\mathcal{R}_{\boldsymbol{W}}(\boldsymbol{V}) = \sqrt{\tilde{\boldsymbol{A}}}^{-1}\,\text{qf}\left(\sqrt{\tilde{\boldsymbol{A}}}(\boldsymbol{W}+\boldsymbol{V})\right), \tag{18}$$

where $\text{qf}(\cdot)$ denotes the function that returns the Q-factor of QR factorization when all the diagonal elements of the R-factor are positive. Note that $\tilde{\boldsymbol{A}}$ as well as $\boldsymbol{A}$ is assumed to be positive definite.

The proposed NLMS algorithm is summarized as an iteration of the following steps, starting with an initial value $\boldsymbol{W}_0 \in \mathcal{M}$:

1) Compute the gradient $\text{grad}\ \sigma_n(\boldsymbol{W}_n)$ in (17).
2) Update $\boldsymbol{W}_{n+1} = \mathcal{R}_{\boldsymbol{W}}(-\mu_n\ \text{grad}\ \sigma_n(\boldsymbol{W}_n))$.

We also update the step size parameter μ_n on the basis of the power of the reference signal $\|\boldsymbol{x}_n\|_2^2$ at each iteration according to (5) as

$$\mu_n = \frac{\mu_0}{2\|\boldsymbol{G}^{\mathsf{H}}\boldsymbol{G} + \gamma\boldsymbol{I}_L\|_2\|\boldsymbol{x}_n\|_2^2}. \tag{19}$$

In the above steps, additional computations after calculating the standard gradient $\partial\sigma_n(\boldsymbol{W})/\partial\boldsymbol{W}^*$, whose computational cost $O(ML + 2LR)$ is equivalent to that of the NLMS algorithm in (4), are necessary at each iteration. The gradient $\text{grad}\ \sigma_n(\boldsymbol{W})$ requires $O(R^3)$ for solving the Sylvester equation (16) [21] and $O(LR^2 + L^2R)$ for the orthogonal projection (15). The retraction (18) requires $O(LR^2)$ for matrix manipulation and $O(R^3)$ for QR factorization. Since the number of reference microphones R is generally small, the increase in the total computational cost from (4) is not large in practice.

V. Numerical Experiments

We conducted numerical experiments to evaluate the performance of the proposed method in terms of noise reduction and exterior radiation suppression in a 2D free field. We compared the NLMS algorithm without exterior radiation suppression (**NLMS**), the NLMS algorithm based on the penalty term [13] (**Ext-Penal NLMS**), and the proposed method based on the Riemannian optimization (**Ext-Riem NLMS**).

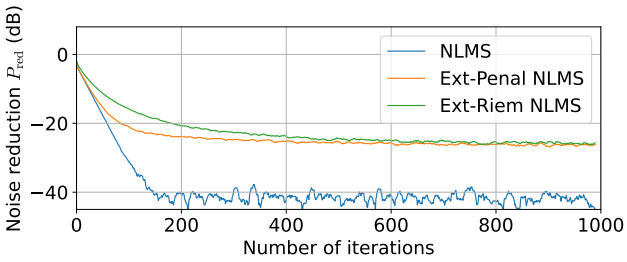

(a) Noise reduction P_{red}

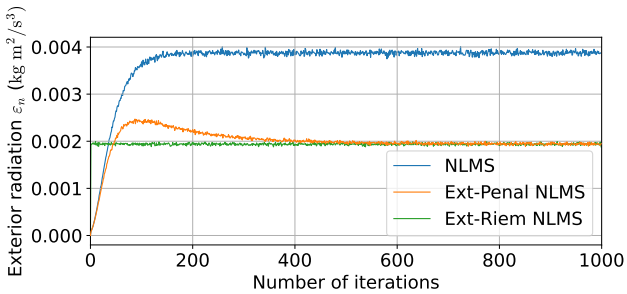

(b) Exterior radiation ε_n

Fig. 3. Noise reduction P_{red} and exterior radiation ε_n at each iteration when the noise frequency was 500 Hz.

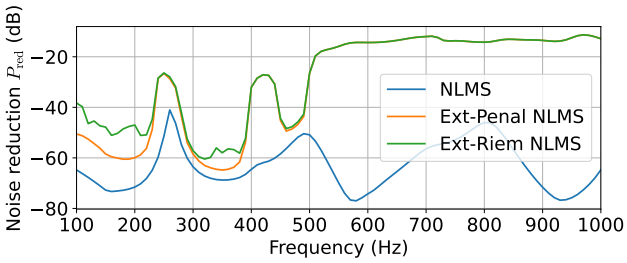

(a) Noise reduction P_{red}

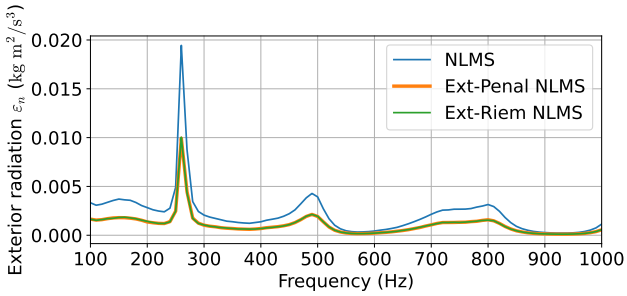

(b) Exterior radiation ε_n

Fig. 4. Noise reduction P_{red} and exterior radiation ε_n after 50000 iterations with respect to frequency.

A. Settings

We assumed that two primary noise sources were placed at $(-3.0, 0.5)$ m and $(3.0, 0.0)$ m. As shown in Fig. 2, $M = 4$ error microphones were set at $(\pm 0.5,\ \pm 0.5)$ m. $L = 12$ secondary loudspeakers were regularly placed at the boundaries of two circular regions with a radius of 1.0 m and 1.2 m. $R = 2$ reference microphones were assumed to directly

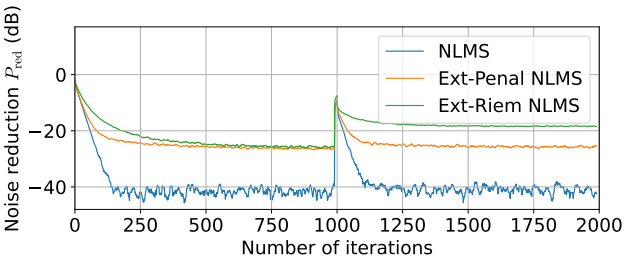

(a) Noise reduction P_{red}

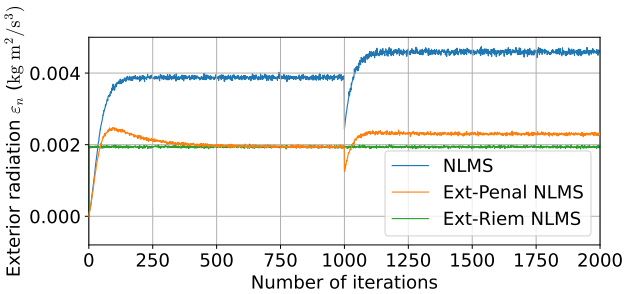

(b) Exterior radiation ε_n

Fig. 5. Noise reduction P_{red} and exterior radiation ε_n at each iteration (500 Hz) when the amplitudes of the primary noise sources changed after 25000 iterations.

and separately obtain the primary noise signals. The primary and secondary sources were assumed to be point sources. The sound speed and medium density were set as $c = 343$ m/s and $\rho = 1.3$ kg/m^3, respectively. We also added Gaussian noise of 40 dB SNR to the reference and error signals at each time frame.

The parameter γ in σ_n was set as the value of 10^{-4} times the maximum eigenvalue of $\boldsymbol{G}^{\mathsf{H}}\boldsymbol{G}$. The normalized step size parameter μ_0 was set to 1.0 for all the methods. The parameters λ in (9) and C in (12) used for the constraint on the exterior radiation power were determined so that the exterior radiation power corresponds to half that obtained by the NLMS algorithm without exterior radiation suppression, i.e., **NLMS**, after convergence. Note that the setting of λ requires exhaustive search as opposed to the setting of C, which can be simply determined from the exterior radiation power of **NLMS**.

In **Ext-Riem NLMS**, the noise at the error microphones can be amplified particularly at the beginning of the adaptation process, because the control filter can be at a point on $\mathcal{M}$. Therefore, $\boldsymbol{d}_n$ and $\boldsymbol{e}_n$ are predicted from $\boldsymbol{x}_n$ before updating $\boldsymbol{W}_n$, and we set $\boldsymbol{y}_n = \boldsymbol{0}$ when $\|\boldsymbol{e}_n\|_2^2 > \|\boldsymbol{d}_n\|_2^2$ is inferred.

As an evaluation measure for the noise reduction at the error microphone positions, we define P_{red} as

$$P_{\mathrm{red}} = \frac{\|\boldsymbol{e}_n\|_2^2}{\|\boldsymbol{d}_n\|_2^2} = \frac{\|\boldsymbol{d}_n + \boldsymbol{G}\boldsymbol{W}_n\boldsymbol{x}_n\|_2^2}{\|\boldsymbol{d}_n\|_2^2}. \tag{20}$$

The exterior radiation suppression is evaluated using ε_n defined in (7). Note that ε_n accurately evaluates the exterior radiation power in this setting since the secondary loudspeakers were assumed to be point sources.

B. Results

Fig. 3 shows the moving averaged P_{red} and ε_n at each iteration when the amplitudes of primary sources were 10.0 and 5.0, respectively, and the frequency was 500 Hz. As shown in Fig. 3(a), P_{red} was successfully reduced in the three methods, and its convergence speed was almost the same, although P_{red} of **Ext-Penal NLMS** and **Ext-Riem NLMS** were higher than that of **NLMS**. Meanwhile, the exterior radiation power ε_n values of **Ext-Penal NLMS** and **Ext-Riem NLMS** after convergence were almost half that of **NLMS** as intended (Fig. 3(b)). In particlar, ε_n was constant at the target value in **Ext-Riem NLMS** from the beginning of the ANC process, excluding the effect of sensor noise.

The evaluation measures after convergence, which were averaged over 100 iterations, with respect to frequency are plotted in Fig. 4. The parameters λ in (9) and C in (12) were determined at each frequency. The noise reduction performance characteristics of the **Ext-Penal NLMS** and **Ext-Riem NLMS** were slightly lower than that of NLMS at low frequencies, but their difference was increased at high frequencies. The exterior radiation powers of **Ext-Penal NLMS** and **Ext-Riem NLMS** were almost half that of **NLMS** for all the frequencies. Note that the exterior radiation power during the adaptation process was explicitly constrained only in **Ext-Riem NLMS**.

Next, we show the result obtained when the amplitude of the primary sources was changed from 10.0 and 5.0 to 5.0 and 10.0 at $n = 1000$ in Fig. 5. Note that $\|\boldsymbol{x}_n\|_2^2$ remained the same after the amplitude change. P_{red} of **NLMS** was smaller than those of **Ext-Penal NLMS** and **Ext-Riem NLMS** at $n = 2000$. The exterior radiation power ε_n was amplified in **NLMS** and **Ext-Penal NLMS** after $n = 1000$. In contrast, ε_n of **Ext-Riem NLMS** remained the same after the amplitude change, which can be considered as an advantage of the Riemannian-optimization-based algorithm.

VI. Conclusion

We proposed a multichannel ANC method for suppressing the exterior radiation of secondary loudspeakers while reducing noise at positions of error microphones. By using a representation of the exterior radiation power by a quadratic of loudspeaker driving signals, we derived an NLMS algorithm based on the Riemannian optimization to update the control filter with the exterior radiation power constrained to a target value. The benefits of the proposed method against the method using a penalty term for the exterior radiation are as follows. 1) The exterior radiation power can be constrained to a target value during the adaptation process. 2) The parameter for the constraint can be set in advance (the exhaustive search for the balancing parameter in the penalty-term-based method is unnecessary). They are also shown in the experimental results. The formulation of the adaptive filtering algorithm for broadband ANC will be a future work.

VII. Acknowledgment

This work was supported by JST FOREST Program (Grant Number JPMJFR216M, Japan), JSPS KAKENHI Grant Number JP22H03608, and Tateisi Science and Technology Foundation.

References

[1] P. A. Nelson and S. J. Elliott, *Active control of sound.* London: Academic Press, 1991.

[2] S. M. Kuo and D. R. Morgan, "Active noise control: a tutorial review," *Proc. IEEE*, vol. 87, no. 6, pp. 943–973, 1999.

[3] Y. Kajikawa, W.-S. Gan, and S. M. Kuo, "Recent advances on active noise control: open issues and innovative applications," *APSIPA Trans. Signal Inf. Process.*, vol. 1, p. e3, 2012.

[4] P. N. Samarasinghe, W. Zhang, and T. D. Abhayapala, "Recent advances in active noise control inside automobile cabins: Toward quieter cars," *IEEE Signal Process. Mag.*, vol. 33, no. 6, pp. 61–73, 2016.

[5] J. Zhang, T. D. Abhayapala, W. Zhang, P. N. Samarasinghe, and S. Jiang, "Active noise control over space: A wave domain approach," *IEEE/ACM Trans. Audio, Speech, Lang. Process.*, vol. 26, no. 4, pp. 774–786, 2018.

[6] F. Ma, W. Zhang, and T. D. Abhayapala, "Active control of outgoing broadband noise fields in rooms," *IEEE/ACM Trans. Audio, Speech, Lang. Process.*, vol. 28, pp. 529–539, 2020.

[7] S. Koyama, J. Brunnström, H. Ito, N. Ueno, and H. Saruwatari, "Spatial active noise control based on kernel interpolation of sound field," *IEEE/ACM Trans. Audio, Speech, Lang. Process.*, vol. 29, pp. 3052–3063, 2021.

[8] B. Rafaely and S. J. Elliot, "A computationally efficient frequency-domain LMS algorithm with constraints on the adaptive filter," *IEEE Trans. Signal Process.*, vol. 48, no. 6, pp. 1649–1655, 2000.

[9] X. Qiu and C. H. Hansen, "A study of time-domain FXLMS algorithms with control output constraint," *J. Acoust. Soc. Amer.*, vol. 109, no. 6, pp. 2815–2823, 2001.

[10] D. Shi, W.-S. Gan, B. Lam, and C. Shi, "Two-gradient direction FXLMS: An adaptive active noise control algorithm with output constraint," *Mech. Syst. Signal Process.*, vol. 116, pp. 651–667, 2019.

[11] D. Shi, W.-S. Gan, B. Lam, S. Wen, and X. Shen, "Optimal output-constrained active noise control based on inverse adaptive modeling leak factor estimate," *IEEE/ACM Trans. Audio, Speech, Lang. Process.*, vol. 29, pp. 1256–1269, 2021.

[12] N. Ueno, S. Koyama, and H. Saruwatari, "Sound field reproduction with exterior radiation cancellation using analytical weighting of harmonic coefficients," in *Proc. IEEE Int. Conf. Acoust., Speech, Signal Process. (ICASSP)*, 2018, pp. 466–470.

[13] K. Arikawa, S. Koyama, and H. Saruwatari, "Kernel-interpolation-based spatial active noise control with exterior radiation suppression," in *Proc. Int. Congr. Acoust. (ICA)*, 2022.

[14] P.-A. Absil, R. Mahony, and R. Sepulchre, *Optimization Algorithms on Matrix Manifolds*. Princeton: Princeton University Press, 2008.

[15] H. Sato, *Riemannian Optimization and Its Applications*. Cham: Springer Nature Switzerland AG, 2021.

[16] S. Bonnabel, "Stochastic gradient descent on Riemannian manifolds," *IEEE Trans. Autom. Control*, vol. 58, no. 9, pp. 2217–2229, 2013.

[17] S. Haykin, *Adaptive Filter Theory: International Edition, 5/E*. London: Pearson, 2013.

[18] B. Shustin and H. Avron, "Preconditioned Riemannian optimization on the generalized stiefel manifold," 2019.

[19] R. A. Horn and C. R. Johnson, *Matrix analysis*. New York: Cambridge University Press, 2012.

[20] H. Sato and K. Aihara, "Cholesky QR-based retraction on the generalized Stiefel manifold," *Comput. Optim. App.*, vol. 72, no. 2, pp. 293–308, 2019. [Online]. Available: https://doi.org/10.1007/s10589-018-0046-7

[21] R. H. Bartels and G. W. Stewart, "Solution of the matrix equation $AX + XB = C$," *Commun. ACM*, vol. 15, no. 9, pp. 820–826, 1972.